Rotational Dynamics of Strongly Adsorbed Solute at the Water Surface†

Mindy L. Johnson, Carlos Rodriguez, and Ilan Benjamin*

Department of Chemistry and Biochemistry, University of California, Santa Cruz, California 95064

Received: October 06, 2008; Revised Manuscript Received: November 30, 2008

The orientational dynamics of nitrobenzene adsorbed at the water liquid/vapor interface as a model for the orientational dynamics of surface-active solute are studied using classical molecular dynamics computer simulations. By varying the charge distribution of the solute and by comparing the results with those in bulk water, we are able to determine the effects of dielectric and mechanical frictions on reorientation dynamics and to correlate the orientational dynamics with the specific hydration of the solute. As in our previous model studies, we find that the equilibrium orientational relaxation is much slower in the bulk than at the interface. Variations of the solute charge distributions show that, as the solute becomes more polar, the surface rotation slows and approaches the bulk behavior. The reorientation dynamics are quite anisotropic, with out-of-plane rotation faster than in-plane rotation. This anisotropy disappears when the solute−water electrostatic interactions are turned off.

I. Introduction

The study of molecular rotation at liquid interfaces in general and at water surfaces in particular is of fundamental importance for understanding the nature of the interface region, especially the concepts of interfacial dielectric and hydrodynamic frictions and their relation to intermolecular solute−solvent interactions.[1−13] The well-established current knowledge about the variations in density, viscosity, and dielectric properties of the interface region[14] on the nanometer length scale, as well as information about hydrogen-bonding structure and dynamics at water surfaces,[15−18] suggests marked effects on the rotational dynamics of solute molecules compared with those in the bulk medium.

Only a few experimental studies of solute reorientation dynamics at liquid surfaces have been published. Several groups have used time-resolved second harmonic generation (SHG) spectroscopy to measure the reorientation dynamics of solute molecules at the water liquid/vapor interface.[19−23] Some of these studies have shown that the time constant for the decay of the SHG signal is slower than the bulk reorientation time as measured by fluorescence anisotropy decay,[19−21,23] and some have suggested the opposite behavior.[22] Even fewer theoretical studies using molecular dynamics simulations have appeared.[24−28] Clearly, many more studies are required to clarify the factors that influence molecular rotations at liquid interfaces. We have recently reported a systematic study of the effect of a diatomic solute location and electric dipole on its reorientation dynamics at the water liquid/vapor interface.[27] It was found that the reduced density at the water surface speeds the reorientational relaxation of a nonpolar solute compared with the dynamics in bulk water. However, as the solute dipole is increased (in the range from 0 to 16 D), the surface rotation slows and approaches that in bulk water. We showed that this is due to the tightening of the solute hydration shell, which makes the local solute environment similar to that in bulk water. Indeed, a high degree of correlation was found between the peak value of the solvent−solute averaged radial distribution function and the rotational relaxation time.

In the present paper we consider the reorientation of a surface-active nonsymmetric molecule. Such a molecule is significantly different from the model diatomic solute previously studied because it is strongly adsorbed at the surface with a specific orientation, introducing an important factor[29,30] which has not been previously considered. As the solute molecule, we chose nitrobenzene, with a NO_2 group as a polar hydrogen-bonding moiety on one end and a hydrophobic benzene ring on the other end. This molecule shares some of the characteristics of dye molecules that have been studied experimentally, and yet it is small enough that its rotation is relatively fast so accurate rotational correlation functions can be determined. In addition, accurate potential energy functions for the water−nitrobenzene interactions have been developed.[31] The study of the reorientation of a strongly adsorbed solute is also motivated by the fact that standard techniques of measuring reorientation dynamics in bulk solution[7] (such as fluorescence anisotropy decay), which are generally not applicable at liquid interfaces because of the weak signal, can be utilized for strongly adsorbed solute at interfaces.[32,33] Our goal is two-fold: (1) to examine to what extent the general finding on the reorientation of simple dipolar solutes mentioned above is applicable here and (2) to examine what, if any, is the effect of the specific adsorbate orientation on its orientational relaxation.

The rest of this paper is organized as follows: In section II, the potential energy functions used and the different systems studied are described, followed by a brief summary of the type of equilibrium correlation functions calculated. In section III, the dynamics and relevant structural results are described and discussed. Conclusions are presented in section IV.

II. Systems and Methods

1. Systems and Potentials. The system under study includes 1000 water molecules and a single nitrobenzene molecule in a rectangular box of dimensions 31.3 Å × 31.3 Å × 100 Å, with the z axis as the long axis of the box. This slab geometry and the use of periodic boundary conditions in all three dimensions give rise to two water liquid/vapor interfaces, whose Gibbs surfaces (where the average water density is near 50% of the bulk value[34]) are at locations of ±14.65 Å. For improved

† Part of the "Max Wolfsberg Festschrift".

10.1021/jp808842k CCC: $40.75
Published on Web 01/21/2009

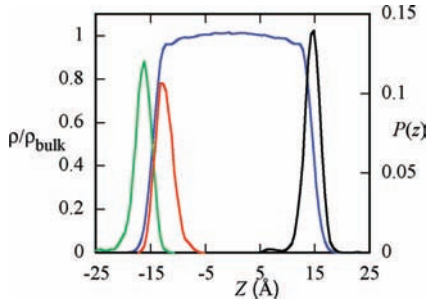

Figure 1. Probability distribution (normalized to unit area) of the nitrobenzene center of mass superimposed on the water density profile (blue curve). The black, green, and red curves correspond to normal nitrobenzene, to a nitrobenzene where its electrostatic interactions with water are switched off, and to the case where they are enhanced by a factor of 2, respectively.

statistics, we utilize both interfaces for the study of the solute rotation. We use a separate truncated octahedron box of size 39.1 Å (of the enclosing cubic box) containing 992 water molecules for the calculation of the orientational dynamics in bulk water. We use a molecule-based switching function at half the box length and a reaction field correction for the long-range electrostatic forces.[35]

The water is modeled using a flexible simple point charge (FSPC) potential, which has been shown to describe reasonably well the interfacial properties of water.[36] The nitrobenzene molecule is described using a flexible, all-atom model with an intramolecular potential based on harmonic bond stretching and bending and a cosine series for the torsion and improper torsion terms.[31] The water−nitrobenzene intermolecular interactions are modeled using the standard Lennard-Jones plus electrostatic terms:

$$u_{ij}(r) = 4\varepsilon_{ij}\left[\left(\frac{\sigma_{ij}}{r}\right)^{12} - \left(\frac{\sigma_{ij}}{r}\right)^{6}\right] + \frac{q_i q_j}{4\pi r \varepsilon_0} \quad (1)$$

where i and j denote atoms on two different molecules separated by a distance r. The Lennard-Jones parameters and the charges for the like-atom interactions are given elsewhere.[31] The Lennard-Jones parameters for the interactions between different atom types are determined from the standard (Lorentz−Berthelot) mixing rules:[37]

$$\sigma_{ij} = (\sigma_{ii} + \sigma_{jj})/2, \quad \varepsilon_{ij} = (\varepsilon_{ii}\varepsilon_{jj})^{1/2} \quad (2)$$

The water−nitrobenzene potential has been extensively tested, and it gives reasonable results for a number of surface properties.[31,38]

The intermolecular potential energy functions used in this work are pairwise additive, so the polarizability of the solvent and solute molecules is included in an average way by proper adjustment of the Lennard-Jones parameters and the point charges. A more accurate approach, which employs many-body polarizable potentials, is more appropriate at the interface.[39−52] This will be described in a future paper using the results given here as a useful comparison.

2. Methods. Figure 1 shows the density profile of water and the probability distribution of the nitrobenzne molecule center of mass from a 2 ns equilibrium trajectory at 298 K. The three distributions shown correspond to normal nitrobenzene and to the cases where the water−nitrobenzene electrostatic interactions are turned off or doubled (more about this later). The distributions clearly demonstrate that the normal solute is strongly adsorbed at the water surface.

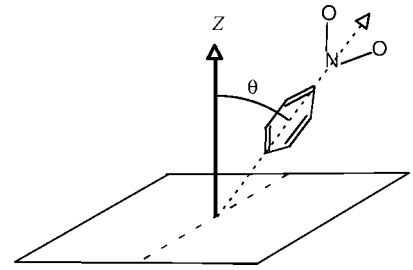

Figure 2. Coordinates for nitrobenzene at the water liquid/vapor interface.

Equilibrium trajectories at a fixed temperature of $T = 298$ K are used to compute the equilibrium orientational correlation functions defined as

$$C_l(t) = \langle P_l[\mathbf{d}(t)\cdot\mathbf{d}(0)]\rangle \quad (3)$$

where $\mathbf{d}(t)$ is a unit vector fixed in the nitrobenzene molecule frame and P_l is the lth-order Legendre polynomial. $C_l(t)$ is, in general, nonexponential, and the corresponding orientational relaxation time is taken as the integral

$$\tau_l = \int_0^\infty C_l(t)\, dt \quad (4)$$

Note that while these correlation functions can be determined experimentally in bulk solutions,[7,13] surface experiments involve more complicated time correlation functions.[53] However, the advantage of $C_l(t)$ is that one can conveniently compare bulk and surface dynamics.

Equation 3 gives identical weights to rotation of the molecule in the surface plane (the XY plane) and to out-of-plane rotation. To examine the separate motions, two other correlation functions are computed. The function $C^{in}(t)$ describes the in-plane equilibrium orientational dynamic:

$$C^{in}(t) = \frac{\langle \mathbf{d}_{xy}(t)\cdot\mathbf{d}_{xy}(0)\rangle}{\langle \mathbf{d}_{xy}\cdot\mathbf{d}_{xy}\rangle} \quad (5)$$

where $\mathbf{d}_{xy}(t)$ is the projection of the solute bond vector $\mathbf{d}$ on the plane parallel to the interface. Note that $C^{in}(0) = 1$ and, as $t \rightarrow \infty$, $\langle \mathbf{d}_{xy}(t)\cdot\mathbf{d}_{xy}(0)\rangle \rightarrow \langle \mathbf{d}_{xy}\rangle^2 = 0$ (due to the cylindrical symmetry of the system) and thus $C^{in}(t) \rightarrow 0$. The projection of $\mathbf{d}$(t) on the direction normal to the interface, $z(t)$, is used to characterize the out-of-plane equilibrium dynamics using the correlation function

$$C^{out}(t) = \frac{\langle z(t)\, z(0)\rangle - \langle z\rangle^2}{\langle z(0)\, z(0)\rangle - \langle z\rangle^2} \quad (6)$$

$C^{out}(0) = 1$, and as $t \rightarrow \infty$, $C^{out}(t) \rightarrow 0$. In a bulk homogeneous medium, $C^{in}(t) = C^{out}(t)$.

All the molecular dynamics simulations were done using a time step of 0.5 fs and the velocity version of the Verlet algorithm.[35]

III. Results and Discussion

In the following, we will consider the reorientation of the vector that passes through the benzene ring and bisects the NO_2 bond angle (see Figure 2).

In condensed media, due to the high solvent−solute collision rate, the solute rotational motion is highly hindered and can be viewed as a succession of very small angle jumps around a randomly oriented axis. This leads to the following result of a simple diffusion model:[1]

$$C_l(t) = \exp[-l(l+1)D_r t] \quad (7)$$

where D_r is a rotational diffusion constant. Thus, $[\ln C_l(t)]/l(l+1)$ vs time should be a straight line with a slope of D_r, independent of l. The rotational correlation time τ_l (eq 4) is thus inversely proportional to D_r. Hydrodynamic models can relate D_r and τ_l to solvent viscosity,[1,7,54] but in general, they are considered parameters that denote the magnitude of the solvent−solute friction.[55]

Figure 3 summarizes our main results. It compares the surface vs the bulk equilibrium reorientation correlation functions $C_1(t)$ and $C_2(t)$ for the main axis of the benzene ring for normal nitrobenzene and for a couple of modifications of the nitrobenzene−water interactions to gain insight into the molecular factors that influence its rotation.

We can make the following observations regarding the reoreintational dynamics of nitrobenzene at the water liquid/vapor interface compared with that in bulk water.

(1) For normal nitrobenzene (unmodified interactions), the bulk behavior is reasonably well described by a simple diffusion. The solid blue curve ($l = 1$) is nearly linear and quite similar to the $l = 2$ curve (blue dotted line), in agreement with eq 7. In contrast, there is substantial deviation from linearity for surface reorientation, and except at early time, the $l(l+1)$ scaling is not obeyed. An examination of individual rotational trajectories shows that at the interface the small-step diffusion motion is interrupted by sudden large-amplitude motion. The reorientation time at the bulk is significantly longer than at the surface: τ_1(bulk) = 29 ± 3 ps, τ_1(surface) = 11 ± 2 ps.

(2) Eliminating the water−nitrobenzene electrostatic interactions reduces the so-called dielectric friction and speeds the rotational relaxation. We now have τ_1(bulk) = 11 ± 1 ps and τ_1(surface) = 1.8 ± 0.2 ps. However, the character of the motion is quite different. In the bulk, there is significant deviation from the $l(l+1)$ scaling relation, while it is nearly perfect at the interface. In fact, the very short relaxation time at the interface suggests that most of the relaxation is taking place in the inertial nondiffusive regime. In this regime, which corresponds to early time prior to the "first" collision between the solute and the solvent molecules, one expects a Gaussian behavior, reflecting free inertial motion:[1]

$$C_l(t) \approx e^{-(kT/2I)l(l+1)t^2}, \quad t < \tau_0 \quad (8)$$

where τ_0 is the free rotation time of the molecule (around 4 ps). Thus, we have $[\ln C_l(t)]/l(l+1) \approx -(kT/2I)t^2$, independent of l, and each panel of Figure 3 shows that, for $t < 4$ ps, the $l = 1$ and $l = 2$ lines coincide.

(3) Doubling the nitrobenzene−water electrostatic interactions increases the dielectric friction and brings the bulk and surface behavior into perfect diffusion behavior. In addition, the bulk and surface relaxation times are nearly identical, so all four curves in the bottom panel fall on top of each other. We have τ_1(bulk) = τ_1(surface) = 63 ± 5 ps.

It is important to keep in mind that while the concept of dielectric friction is quite useful and several approximate analytical expressions for it have been developed for continuum solvent models,[2,3,5,7,54,56−59] typically one cannot simply separate it from hydrodynamic friction, especially when there are strong electrostatic interactions. Strong electrostatic interactions can lead to a tightening of the hydration shell (electrostriction) and may significantly increase the hydrodynamic friction.[55]

The fact that there is a close relationship between the structure of the solute hydration shell and the rotational relaxation time has been demonstrated by us previously for a dipolar solute

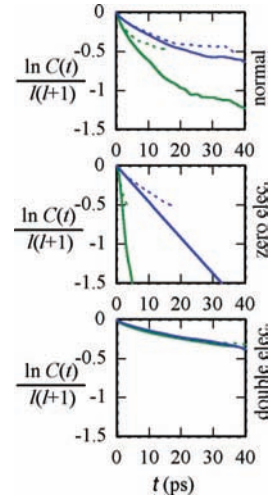

Figure 3. Equilibrium correlation functions for the reorientation of nitrobenzene in bulk and surface water. In each panel are plotted $[\ln C_l(t)]/(l(l+1))$ vs t for the $l = 1$ (solid lines) and $l = 2$ (dotted lines) correlations for nitrobenzene in bulk water (blue) and at the water surface (green). The top panel corresponds to normal nitrobenzene, while the middle and bottom panels correspond to nitrobenzene in which the electrostatic interactions with water are switched off and doubled, respectively. Note that $C_l(t)$ values of less than 0.05 are statistically unreliable and too noisy to show.

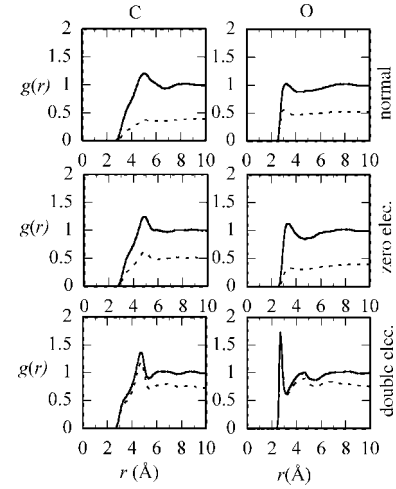

Figure 4. Bulk (solid curves) vs surface (dotted curves) water--nitrobenzene radial distribution functions. The panels on the left and on the right depict the radial distribution function for the water oxygen with the 1-carbon of nitrobenzene (the carbon bonded to the nitro group) and the oxygen of the nitro group, respectively. The top, middle, and bottom panels correspond to normal nitrobenzene and to nitrobenzene in which the electrostatic interactions with water are switched off and doubled, respectively.

with a large dipole. Despite the fact that we have here a hydrophobic solute, the situation is quite similar, as is shown in Figure 4.

Unlike the case of a dipolar solute, the solute here is quite hydrophobic, which is reflected in the modest hydration structure near the carbon atom in bulk water (this structure is even less pronounced in the case of the para carbon atom). The peak is almost not affected by removing the electrostatic interactions and only insignificantly gets larger when the electrostatic interactions are doubled in size. The effect on the (orientationally averaged) radial distribution at the surface is more significant. While for normal nitrobenzene and for nitrobenzene whose electrostatic interactions with water are turned off the interfacial peak is about half the peak in the bulk, the doubling of the

electrostatic interactions brings the two peaks very close to each other. All this is more markedly apparent when one examines the water structure around the oxygen of the nitro group. In particular, when the electrostatic interactions are doubled, the O(water)−O(nitro) radial distribution function in the bulk and at the interface shows prominent identical peaks correlating nicely with the identical rotational relaxation. The oxygen atoms of the nitro group are able to hydrogen bond with water and significantly slow the solute rotation. Eliminating these hydrogen bonds or strengthening them is therefore expected to manifest itself in the rotational relaxation time. The ratio of the peak value of $g_{OO}(r)$ in the bulk vs the interface for the three systems (in the order normal, uncharged, and double charges)—1.9:3.5:1.0—is qualitatively similar to that for the bulk vs surface relaxation time, 2.6:6.0:1.0.

While the radial distribution functions clearly demonstrate that the local solvent environment around the doubly charged solute is similar in the bulk and at the interface, it is worth examining the location of the solute in relation to the interfacial water molecules. The density profile shown in Figure 1 gives only the probability distribution of the solute molecule in relation to the average water density, and while it suggests that the solute is hydrated by surface molecules, it would be useful to identify these more precisely.

The liquid/vapor interface far from the critical temperature (as well as the liquid/liquid interface) can be viewed as an intrinsic surface, $z = \zeta(\mathbf{s})$, $\mathbf{s} = (x, y)$, separating the two bulk phases broadened by thermal density fluctuations.[60] In recent years, a number of authors have suggested ways to define the intrinsic surface and thus identify the surface molecules.[61−67] Of particular utility has been the intrinsic density profile defined as[63−67]

$$\rho_{\text{int}}(z) = \left\langle \frac{1}{A}\sum_{i=1}^{N} \delta(z - z_i + \zeta(\mathbf{s})) \right\rangle \tag{9}$$

where A is the surface area and the sum is over all the N solvent molecules. If one takes the intrinsic surface to be a constant, one recovers the mean density profile.

To examine the density distribution of water molecules along the interface normal in relation to a particular atomic site on the nitrobenzene molecule, we consider analogously to eq 9 the following expression:

$$\rho_k(z) = \left\langle \frac{1}{A}\sum_{i=1}^{N'} \delta(z - z_i + z_k) \right\rangle \tag{10}$$

where z_k is the location along the surface normal of one of the nitrobenzene atoms. Since we are interested in the water molecules in the vicinity of the solute, the sum in eq 10 is over all the water molecules in a cylinder of a radius equal to the hydration shell radius R_k of this atom: $(x_i - x_k)^2 + (y_i - y_k)^2 \leq R_k^2$, where (x_i, y_i, z_i) is the position of the oxygen atom of the ith water molecule. There is no restriction on the z position of the water molecules, except for removing any vapor-phase molecule that is inside the cylinder defined above (a very rare occurrence).

Figure 5 shows the results of the intrinsic water density profiles (normalized to 1 in bulk water) calculated according to eq 10 for the 1-carbon and the oxygen atoms of nitrobenzene. The densities for the two oxygen atoms are nearly identical, so they are averaged together. Note that $z = 0$ corresponds to the location of the solute atom, with respect to which the density is calculated. This figure is, in general, consistent with the information provided by the mean density profile, the solute distribution of Figure 1, and the radial distribution functions in Figure 4. It is clear that, in all three cases, the nitrobenzene atoms are above the center of the top layer of water molecules. However, while in the case of the normal and zero charged solute the C and O atoms are near the tail of the profile, there is substantial overlap between the top water layer and the doubly charged solute. Note also the significant perturbation of the water density around the oxygen atoms of the doubly charged nitro group, consistent with the significant peak observed in $g(r)$.

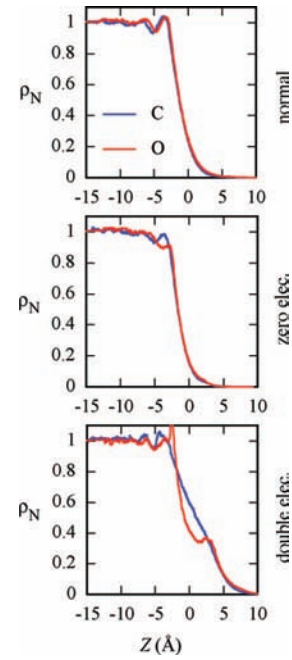

Figure 5. Intrinsic water density profile (normalized by the bulk value) in relation to the location of the 1-carbon atom and the oxygen atoms of nitrobenzene located at the water liquid/vapor interface. The top, middle, and bottom panels correspond to normal nitrobenzene and to nitrobenzene in which the electrostatic interactions with water are switched off and doubled, respectively.

An additional new feature presented by nitrobenzene rotation at the water surface is the fact that this solute has a well-defined orientation at the surface with a barrier for complete flipping of the molecule. The NO_2 group prefers to point toward bulk water by forming hydrogen bonds, as was demonstrated in studies of the water/nitrobenzene liquid/liquid interface.[31,38] In addition, the planar nature of the molecule also suggests that information about the orientation of this plane with respect to the surface normal would be useful. The orientation of this plane can be specified by the angle between the surface normal and any vector that lies in the plane of the benzene ring (or perpendicular to it). We take this to be the vector connecting the two ortho carbon atoms, and we denote the angle by ϕ. As shown by Jedlovszky et al.,[68] the bivariate distribution $P(\theta,\phi)$ that gives the joint probability of the pair of angles θ and ϕ should be used for a complete specification of the molecular orientation. This distribution is given in Figure 6.

This figure shows that the main axis of normal nitrobenzene forms an angle of 110° with respect to the surface normal, with the NO_2 group pointing toward bulk water. The plane of the ring is nearly perpendicular to the surface normal. However, the distribution is quite broad. Removing the water−nitrobenzene electrostatic interactions results in the molecule preferring to lie flat on the surface. Doubling the electrostatic interactions, significantly enhancing the water−NO_2 group hydrogen bonding (as is clear from $g(r)$), gives rise to a significant sharpening of

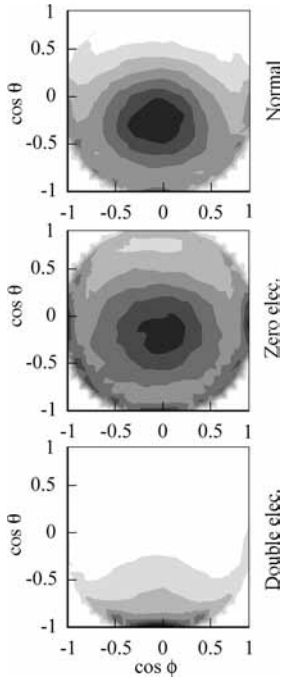

Figure 6. Bivariate orientational probability distribution for nitrobenzene at the water liquid/vapor interface. θ was defined in Figure 2, and ϕ is the angle between the surface normal and the vector connecting the two ortho carbon atoms. In each panel, the darkest color corresponds to the peak value of the distribution. The top, middle, and bottom contour plots correspond to normal nitrobenzene and to a nitrobenzene where its electrostatic interactions with water are switched off and doubled, respectively.

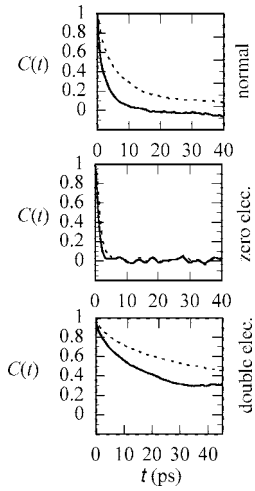

Figure 7. Equilibrium anisotropic orientational correlation functions for nitrobenzene at the water liquid/vapor interface. In each panel, the solid and dashed lines depict C^{out} (eq 6) and C^{in} (eq 5), respectively.

the orientational distribution function. The orientational distribution now is peaked around $\theta = 160°$ from the surface normal, with a much larger barrier for a complete flipping of the molecule. Of course when the main axis of the molecule is perfectly normal to the surface ($\cos\theta = -1$), the benzene ring must be perpendicular to the normal and $\cos\phi = 0$.

The difference in the solute−solvent interactions also manifests itself in the orientational dynamics. Figure 7 shows the results for the correlation functions defined in eqs 5 and 6 for the in-plane and out-of-plane motion, respectively. The in-plane reorientational dynamics are very similar to the dynamics described by the C_1 correlation functions shown earlier. We see that, for both normal nitrobenzene and nitrobenzene with double electrostatic interaction with water, the out-of-plane dynamics is faster than the in-plan dynamics. However, an examination of the rotational trajectories shows that the reorientation of normal nitrobenzene involves some infrequent rapid tilting of the angle θ, while the motion of the nitrobenzene with the stronger electrostatic interactions is more of a small angle diffusion in a cone centered around the most probable orientation. Thus, the rapid out-of-plane dynamics does not represent large jumps in θ. In contrast, when the water−nitrobenzene interactions are turned off, the reorientation dynamics are quite isotropic. These results are similar to the behavior of a dipolar solute at the water liquid/vapor interface[27] and are also consistent with the experimental data[21] and simulations[26] for coumarin-314 at the air/water interface.

It is interesting to contrast these observations with the translational and rotational dynamics at water/organic liquid interfaces. Calculations at the water/nitrobenzene interface,[31,38] water hydrocarbon interfaces,[65] and other liquid/liquid interfaces[14] generally show that rotation and translation perpendicular to the interface are slower than motion in the interface plane, due to the existence of a well-defined surface layer. The situation here is quite different, since out-of-plane motion brings part of the molecule into the low-density "vapor" region, which speeds the dynamics.

IV. Conclusions

The reorientation dynamics of nitrobenznene (as an example of a surface-active solute) at the water liquid/vapor interface is controlled by the local solvent density and by the solute charge distributions. Nitrobenzene orientational relaxation is *faster* at the interface than in the bulk due to lower local water density and thus smaller hydration and effective friction. This is reflected in the significant reduction in the surface (orientationally averaged) radial distribution functions compared with the bulk ones and in the location of the solute relative to the water surface layer. While removing the water−nitrobenznene electrostatic interactions does not change this result, doubling these interactions significantly increases the rotational friction and slows the surface relaxation, resulting in dynamics that are very similar to the bulk dynamics. This behavior strongly correlates with the peak value of the water−nitrobenzene radial distribution function, which is almost identical in the bulk and at the interface. The orientational correlation functions agree well with rotational diffusion models in this case, but deviations are observed for the normal solute at the water surface.

The electrostatic solute−solvent interactions contribute to the specific orientational preference of the adsorbed solute and its anisotropic dynamics. The out-of-plane dynamics of normal nitrobenzene and the nitrobenzene with enhanced electrostatic interactions with water are faster than the in-plane motion, but removing the electrostatic interactions results in a fairly isotropic relaxation.

Acknowledgment. This work has been supported by a grant from the National Science Foundation (CHE-0809164). Discussions with Prof. Richard Stratt about anisotropic correlation functions are gratefully acknowledged.

References and Notes

(1) Steele, W. A. *Adv. Chem. Phys.* **1976**, *34*, 1.
(2) Hynes, J. T.; Kapral, R.; Weinberg, M. *J. Chem. Phys.* **1977**, *67*, 3256.
(3) Dote, J. L.; Kivelson, D.; Schwartz, R. N. *J. Phys. Chem.* **1981**, *85*, 2169.

(4) *Molecular Liquids Dynamics and Interactions*; Barnes, A. J., Orville-Thomas, W. J., Yarwood, J., Eds.; Reidel: Dordrecht, The Netherlands, 1984.
(5) van der Zwan, G.; Hynes, J. T. *J. Phys. Chem.* **1985**, *89*, 4181.
(6) Wang, C. H. *Spectroscopy of Condensed Media*; Academic Press: New York, 1985.
(7) Fleming, G. R. *Chemical Applications of Ultrafast Spectroscopy*; Oxford University: New York, 1986.
(8) Berne, B. J.; Pecora, R. *Dynamic Light Scattering*; Robert E. Krieger: Malabar, FL, 1990.
(9) Hu, Y.; Fleming, G. R. *J. Chem. Phys.* **1991**, *94*, 3857.
(10) Polson, J. M.; Fyfe, J. D. D.; Jeffrey, K. R. *J. Chem. Phys.* **1991**, *94*, 3381.
(11) Cho, M.; Rosenthal, S. J.; Scherer, N. F.; Ziegler, L. D.; Fleming, G. R. *J. Chem. Phys.* **1992**, *96*, 5033.
(12) Chang, Y. J.; Castner, E. W. *J. Chem. Phys.* **1993**, *99*, 113.
(13) Burshtein, A. I.; Temkin, S. I. *Spectroscopy of Molecular Rotation in Gases and Liquids*; Cambridge University Press: Cambridge, U.K., 1994.
(14) Benjamin, I. *Chem. Rev.* **1996**, *96*, 1449.
(15) Du, Q.; Freysz, E.; Shen, Y. R. *Science* **1994**, *264*, 826.
(16) Richmond, G. L. *Chem. Rev.* **2002**, *102*, 2693.
(17) Liu, P.; Harder, E.; Berne, B. J. *J. Phys. Chem. B* **2005**, *109*, 2949.
(18) Benjamin, I. *J. Phys. Chem. B* **2005**, *109*, 13711.
(19) Castro, A.; Sitzmann, E. V.; Zhang, D.; Eisenthal, K. B. *J. Phys. Chem.* **1991**, *95*, 6752.
(20) Eisenthal, K. B. *J. Phys. Chem.* **1996**, *100*, 12997.
(21) Zimdars, D.; Dadap, J. I.; Eisenthal, K. B.; Heinz, T. F. *J. Phys. Chem. B* **1999**, *103*, 3425.
(22) Antoine, R.; Tamburello-Luca, A. A.; Hebert, P.; Brevet, P. F.; Girault, H. H. *Chem. Phys. Lett.* **1998**, *288*, 138.
(23) Nguyen, K. T.; Shang, X.; Eisenthal, K. B. *J. Phys. Chem. B* **2006**, *110*, 19788.
(24) Raghavan, K.; Foster, K.; Motakabbir, K.; Berkowitz, M. *J. Chem. Phys.* **1991**, *94*, 2110.
(25) Benjamin, I. *J. Chem. Phys.* **1991**, *95*, 3698.
(26) Pantano, D. A.; Laria, D. *J. Phys. Chem. B* **2003**, *107*, 2971.
(27) Benjamin, I. *J. Chem. Phys.* **2007**, *127*, 204712.
(28) Benjamin, I. *J. Phys. Chem. C* **2008**, *112*, 8969.
(29) Raising, T.; Shen, Y. R.; Kim, M. W.; Valint, P.; Bock, J *Phys. Rev. A* **1985**, *31*, 537.
(30) Higgins, D. A.; Corn, R. M. *J. Phys. Chem.* **1993**, *97*, 489.
(31) Michael, D.; Benjamin, I. *J. Electroanal. Chem.* **1998**, *450*, 335.
(32) Wirth, M. J.; Burbage, J. D. *J. Phys. Chem.* **1992**, *96*, 9022.
(33) Laia, C. A. T.; Costa, S. M. B. *Langmuir* **2002**, *18*, 1494.
(34) Rowlinson, J. S.; Widom, B. *Molecular Theory of Capillarity*; Clarendon: Oxford, U.K., 1982.
(35) Allen, M. P.; Tildesley, D. J. *Computer Simulation of Liquids*; Clarendon: Oxford, U.K., 1987.
(36) Benjamin, I. Molecular dynamics simulations in interfacial electrochemistry. In *Modern Aspects of Electrochemistry*; Bockris, J. O. M., Conway, B. E., White, R. E., Eds.; Plenum Press: New York, 1997; Vol. 31, p 115.
(37) Hansen, J.-P.; McDonald, I. R. *Theory of Simple Liquids*, 2nd ed.; Academic: London, 1986.
(38) Jorge, M.; Cordeiro, M. N. D. S. *J. Phys. Chem. C* **2007**, *111*, 17612.
(39) Sprik, M.; Klein, M. L. *J. Chem. Phys.* **1988**, *89*, 7556.
(40) Ahlstrom, P.; Wallqvist, A.; Engstrom, S.; Jonsson, B. *Mol. Phys.* **1989**, *68*, 563.
(41) Wallqvist, A. *Chem. Phys.* **1990**, *148*, 439.
(42) Dang, L. X.; Rice, J. E.; Caldwell, J.; Kollman, P. A. *J. Am. Chem. Soc.* **1991**, *113*, 2481.
(43) Smith, D. E.; Dang, L. X. *J. Chem. Phys.* **1994**, *100*, 3757.
(44) Bader, J. S.; Berne, B. J. *J. Chem. Phys.* **1996**, *104*, 1293.
(45) Morita, A.; Kato, S. *J. Chem. Phys.* **1998**, *109*, 5511.
(46) Small, D. W.; Matyushov, D. V.; Voth, G. A. *J. Am. Chem. Soc.* **2003**, *125*, 7470.
(47) Wallqvist, A. *Chem. Phys. Lett.* **1990**, *165*, 437.
(48) Motakabbir, K.; Berkowitz, M. *Chem. Phys. Lett.* **1991**, *176*, 61.
(49) Chang, T. M.; Dang, L. X. *J. Chem. Phys.* **1996**, *104*, 6772.
(50) Benjamin, I. *Chem. Phys. Lett.* **1998**, *287*, 480.
(51) Dang, L. X.; Chang, T. *J. Phys. Chem. B* **2002**, *106*, 235.
(52) Jungwirth, P.; Tobias, D. J. *J. Phys. Chem. A* **2002**, *106*, 379.
(53) Stratt, R. Private communication.
(54) Debye, P. *Polar Molecules*; Dover: New York, 1945.
(55) Horng, M.-L.; Gardecki, J. A.; Maroncelli, M. *J. Phys. Chem. A* **1997**, *101*, 1030.
(56) Nee, T. W.; Zwanzig, R. *J. Chem. Phys.* **1970**, *52*, 6353.
(57) Hu, C.; Zwanzig, R. *J. Chem. Phys.* **1974**, *60*, 4354.
(58) Alavi, D. S.; Waldeck, D. H. *J. Chem. Phys.* **1991**, *94*, 6196.
(59) Alavi, D. S.; Waldeck, D. H. *J. Chem. Phys.* **1993**, *98*, 3580.
(60) Percus, J. K.; Williams, G. O. The intrinsic interface. In *Fluid Interfacial Phenomena*; Croxton, C. A., Ed.; Wiley: New York, 1986; p 1.
(61) Benjamin, I. Molecular dynamics methods for studying liquid interfacial phenomena. In *Modern Methods for Multidimensional Dynamics Computations in Chemistry*; Thompson, D. L., Ed.; World Scientific: Singapore, 1998; p 101.
(62) Ashbaugh, H. S.; Pratt, L. R.; Paulaitis, M. E.; Clohecy, J.; Beck, T. L. *J. Am. Chem. Soc.* **2005**, *127*, 2808.
(63) Chacón, E.; Tarazona, P.; Alejandre, J. *J. Chem. Phys.* **2006**, *125*, 014709.
(64) Chowdhary, J.; Ladanyi, B. M. *J. Phys. Chem. B* **2006**, *110*, 15442.
(65) Chowdhary, J.; Ladanyi, B. M. *J. Phys. Chem. B* **2008**, *112*, 6259.
(66) Pa'rtay, L. B.; Hantal, G.; Jedlovszky, P.; Vincze, A.; Horvai, G. *J. Comput. Chem.* **2008**, *29*, 945.
(67) Jorge, M.; Cordeiro, M. N. D. S. *J. Phys. Chem. B* **2008**, *112*, 2415.
(68) Jedlovszky, P.; Vincze, Á.; Horvai, G. *J. Chem. Phys.* **2002**, *117*, 2271.

JP808842K